A numerical study on heat transport in turbulent Couette flows in concentric annuli

Shuichi Torii
Department of Mechanical Engineering, Kagoshima University, Kagoshima, Japan and
Wen-Jei Yang
Department of Mechanical Engineering and Applied Mechanics, University of Michigan, Ann Arbor, Michigan, USA

Received January 1995
Revised March 1996

Nomenclature

C_p	=	Specific heat at constant pressure, J/kgK
C_μ, C_1, C_2, C_λ, C_{P1}, C_{P2}, C_{D1}, C_{D2}	=	Empirical constants of k–ε model Turbulence model constants for temperature field
D	=	Hydraulic diameter of the annulus, 2 (R_{out}-R_{in}), m
f	=	Friction coefficient
f_μ, f_1, f_2	=	Turbulence model functions of k–ε model
f_λ, f_{P1}, f_{P2}, f_{D1}, f_{D2}	=	Turbulence model functions of temperature field
k	=	Turbulent kinetic energy, m^2/s^2
N	=	Dimensionless relative velocity, U/u_m
Nu	=	Nusselt number
Nu_o	=	Nu for Stationary inner cylinder
$\bar{P}$	=	Time-averaged pressure, Pa
Pr	=	Prandtl number
Pr_t	=	Turbulent Prandtl number
q	=	Heat flux, W/m^2
r	=	Radial co-ordinate, m
Re	=	Reynolds number defined as $2u_m$ (R_{out}-R_{in})/ν
R_{in}	=	Inner radius of the annulus, m
R_{out}	=	Outer radius of the annulus, m
R_t	=	Turbulent Reynolds number, $k^2/\varepsilon\nu$
St	=	Stanton number, $q_w/\rho c_p u_m(\bar{T}_w-\bar{T}_b)$
$\bar{T}$	=	Time-averaged temperature, °K
$T+$	=	Dimensionless time-averaged temperature, $(\bar{T}w-\bar{T})/(q_w/\rho c_p u^*)$
t'	=	Fluctuating temperature component, °K
t^*	=	Friction temperature, $q_w/\rho c_p u^*$, °K
$\overline{t^2}$	=	Temperature variance, $°K^2$
U	=	Velocity of moving inner cylinder, m/s
u_m	=	Mean axial velocity across annular space, m/s
$\bar{u}$, $\bar{v}$	=	time-averaged velocity components in axial and radial directions, respectively, m/s
u', v'	=	Fluctuating velocity components in axial and radial directions, respectively, m/s
u^*	=	Friction velocity, m/s
$u+$	=	Dimensionless velocity, $\bar{u}/u^*$
x	=	Axial co-ordinate, m
y	=	Distance from wall, m
$y+$	=	Dimensionless distance, u^*y/ν

Greek letters

ρ	=	Density, kg/m^3
ε	=	Turbulent energy dissipation rate, m^2/s^3
ε_t	=	Dissipation rate of $\overline{t^2}$, $°K/s^2$
α, α_t	=	Molecular and turbulent thermal diffusivities, respectively, m^2/s
ν, ν_t	=	Molecular and turbulent viscosities, respectively, m^2/s
λ	=	Molecular thermal conductivity, W/mK
σ_k, σ_ε, σ_h, σ_ϕ	=	Turbulence model constants for diffusion of k, ε, t^2 and ε_t, respectively

Subscripts

b	=	Bulk
in	=	Inner side
max	=	Maximum
o	=	Stationary inner cylinder
w	=	Wall
out	=	Outer side

Superscripts

-	=	Time-averaged value
'	=	Fluctuation value

International Journal of Numerical Methods for Heat & Fluid Flow
Vol. 7 No. 1, 1997, pp. 81-94.

Introduction

Annular flow geometries are encountered in many important engineering applications. The problems of heat transfer and fluid flow can be classified into three categories:

(1) stationary cylinder case;

(2) circular Couette flow case; and

(3) parallel Couette flow case.

The first category includes propulsion systems, heat exchangers, and fuel assemblies in nuclear reactors. Turbulent transport phenomena in parallel flow through an annulus between two stationary concentric cylinders with and without heat transfer are reported by many investigators (for example, Brighton and Jones[1], Kays and Leung[2], Heikal *et al.*[3], Fujii *et al.*[4], Torii *et al.*[5]). The circular Couette flow, i.e. swirling flow, implies a flow with one surface rotating and the other stationary (or both surfaces rotating in the same direction at different angular velocities). Problems involving transport phenomena in swirling flows can be found in chemical and mechanical mixing or separation devices, electric and turbo machinery, combustion chambers, pollution control devices, swift nozzles, and fusion reactors. Kuzay and Scott[6,7] investigated concentric annular flows with a rotating or stationary inner cylinder, in which axial and radial temperature profiles are measured. Hirai *et al.*[8] analysed the effect of the axially rotating inner cylinder on the turbulence structures using the Reynolds stress model. Torii and Yang[9] predicted a substantial enhancement in heat transfer performance due to a rotation of the inner cylinder by means of k-ε turbulence models. The parallel Couette flow refers to a flow in a concentric annulus with one surface moving in the flow direction and the other remaining stationary (or both surfaces moving in the flow direction at different velocities). This type flow is seen in railway tunnels such as the 54km-long Seikan tunnel in Japan and the English Channel tunnel. The present study is focused on heat transport phenomena in parallel Couette flows.

To the authors' knowledge, there are no experimental data pertinent to flow characteristics such as the velocity distribution and the turbulence quantities in the annulus for the parallel Couette flow case. In contrast, numerical studies have been conducted to determine fluid flow and heat transfer induced by the streamwise movement of the inner cylinder. Barrow and Pope[10] conducted a simple analysis simulating fluid flow and heat transfer in long railway tunnels. Lee and Kim[11] studied an inverted annular film boiling during an emergency core cooling of nuclear fuel channels, which involves similar fluid flow and heat transfer phenomena. Recently, Shigeehi *et al.*[12] and Torii and Yang[13] obtained analytical solutions for friction factor and Nusselt number for turbulent fluid flow and heat transfer in concentric annuli with a moving inner core, using a modified mixing length model and k-ε turbulence models, respectively. Moreover, Toni and Yang[14] analysed turbulent Couette flow and heat transfer in annuli by means of the turbulent Prandtl number and the Reynolds stress turbulence model of Launder and Shima[15], and investigated the effects of inner

core movement on the flow structure. It was disclosed that in the region near the inner core, a reduction in the velocity gradient induced by its streamwise movement suppresses three normal components of the Reynolds stress and its off-diagonal one, resulting in a decrease in the heat transfer performance.

Throughout the numerical simulations pertinent to the above turbulent heat transport problems, the turbulent heat flux in the energy equation is modelled by using the classical Boussinesq approximation. The unknown turbulent thermal diffusivity α_t is obtained from the definition of the known turbulent viscosity ν_t and the turbulent Prandtl number Pr_t as $\alpha_t = \nu_t/Pr_t$. In this formulation, an analogy between eddy diffusivities of momentum and heat is implicitly assumed. However, shear flow measurements[16] and direct simulation data[17] reveal that its analogy, as represented by the turbulent Prandtl number, cannot adequately reflect the physical phenomenon of heat transport and there are no universal values of turbulent Prandtl number even in simple flows. In order to obtain detailed information on heat transport phenomena, such as temperature fluctuations and turbulent heat flux, the one- and two-equation models for thermal field and the turbulent heat flux equation model are employed in the present study.

It is preferred that the turbulent heat-flux equation model is more universal with Reynolds stresses being closely related to the turbulent heat flux equation. With rapid advances in computers and direct numerical simulation method, a substantial progress has been made in the modelling of the Reynolds stress transport equations: For example, Torii and Yang[14] disclosed the mechanism of transport phenomena in concentric annuli with the inner core moving in the flow direction, as mentioned above. Although the second momentum transport equations can be derived in exact forms, the high-order correlations require some unverified assumptions, in which the principles and basic techniques used in the modelling have not yet been established, particularly in the near-wall region. Furthermore, since a set of non-linear, coupled differential equations for each individual component of the Reynolds stress tensor are simultaneously solved, the numerical computation may sometimes become unstable. Since heat flux transport is much sensitive to time scales than momentum transport[18], it is more difficult to achieve closure of the turbulent heat flux equations than the Reynolds stress equations. Therefore, the modelling of the scalar field is still at its infancy.

The purpose of the present study is to investigate a turbulent fluid flow and heat transfer in a concentric annulus with the inner core moving in the flow direction. The two-equation model for heat transfer proposed by Nagano and Kim[19] is employed to determine the mechanism of the heat transport phenomena. The model approximates the turbulent thermal diffusivity using the temperature variance and the dissipation rate of temperature fluctuations together with the turbulent kinetic energy and its dissipation rate. Emphasis is placed on the effects of inner core movement on the thermal field, i.e. temperature profile, turbulent heat flux and temperature variance.

Governing equations

A turbulent flow in concentric annuli with a slightly heated inner cylinder moving in the flow direction, as shown in Figure 1, is analysed using cylindrical

co-ordinates. The boundary layer approximation is employed to express the steady, two-dimensional, continuity, momentum and energy equations as

$$\frac{\partial \bar{u}}{\partial x}+\frac{\partial \bar{v}}{\partial r}+\frac{\bar{v}}{r}=0 \tag{1}$$

$$\bar{u}\frac{\partial \bar{u}}{\partial x}+\bar{v}\frac{\partial \bar{u}}{\partial r}=-\frac{1}{\rho}\frac{d\bar{P}}{dx}+\frac{1}{r}\frac{\partial}{\partial r}\left(r\nu\frac{\partial \bar{u}}{\partial r}-r\overline{u'v'}\right) \tag{2}$$

$$\bar{u}\frac{\partial \bar{T}}{\partial x}+\bar{v}\frac{\partial \bar{T}}{\partial r}=\frac{1}{r}\frac{\partial}{\partial r}\left(r\alpha\frac{\partial \bar{T}}{\partial r}-r\overline{v't'}\right) \tag{3}$$

,

respectively. The Reynolds stress $-\overline{u'v'}$ and the turbulent heat flux $-\overline{v't'}$ in equations (2) and (3) are obtained using the Boussinesq approximation as:

$$-\overline{u'v'}=\nu_t\frac{\partial \bar{u}}{\partial r} \tag{4}$$

$$-\overline{v't'}=\alpha_t\frac{\partial \bar{T}}{\partial r} \tag{5}$$

,

respectively. Here, the turbulent viscosity vt can be expressed in terms of the turbulent kinetic energy k and its dissipation rate ε, through the Kolmogorov-Prandtl's relation[20], as

$$\nu_t=C_\mu f_\mu\frac{k^2}{\varepsilon} \tag{6}$$

.

C_μ and f_μ are a model constant and a model function, respectively. The turbulent thermal diffusivity α_t is related to the temperature variance $\bar{t}^2$, the dissipation rate of temperature fluctuations ε_t, k and ε as

$$\alpha_t=C_\lambda f_\lambda k\sqrt{\frac{\bar{t}^2}{\varepsilon\varepsilon_t}} \tag{7}$$

,

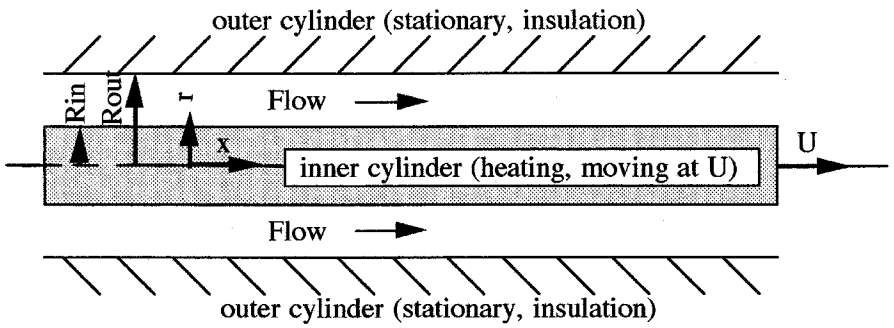

Figure 1.
A schematic of physical system and co-ordinate

where C_λ is a model constant and f_λ is a model function.

The low Reynolds number version of a k-ε turbulence model proposed by Nagano and Hishada[21] reads

$$\bar{u}\frac{\partial k}{\partial x}+\bar{v}\frac{\partial k}{\partial r}=\frac{1}{r}\frac{\partial}{\partial r}\left\{r\left(\frac{\nu_t}{\sigma_k}+\nu\right)\frac{\partial k}{\partial r}\right\}+\nu_t\left(\frac{\partial \bar{u}}{\partial r}\right)^2-\varepsilon-2\nu\left(\frac{\partial \sqrt{k}}{\partial r}\right)^2 \quad (8)$$

$$\bar{u}\frac{\partial \varepsilon}{\partial x}+\bar{v}\frac{\partial \varepsilon}{\partial r}=\frac{1}{r}\frac{\partial}{\partial r}\left\{r\left(\frac{\nu_t}{\sigma_\varepsilon}+\nu\right)\frac{\partial \varepsilon}{\partial r}\right\}+C_1 f_1\frac{\varepsilon}{k}\nu_t\left(\frac{\partial \bar{u}}{\partial r}\right)^2-C_2 f_2\frac{\varepsilon^2}{k}+\nu\nu_t(1-f_\mu)\left(\frac{\partial^2 \bar{u}}{\partial r\partial r}\right)^2 \quad (9)$$

The empirical constants and model functions in equations (6), (8) and (9) are summarized in Table I.

The two-equation heat-transfer model developed by Nagano and Kim[19] is used to obtain $\overline{t^2}$ and ε_t in equation (7), in the present study. The model can accurately predict various thermal fields in the vicinity of the wall as well as in the region far from the wall. The transport equations for $\overline{t^2}$ and ε_t are

$$\bar{u}\frac{\partial \overline{t^2}}{\partial x}+\bar{v}\frac{\partial \overline{t^2}}{\partial r}=\frac{1}{r}\frac{\partial}{\partial r}\left\{r\left(\frac{\alpha_t}{\sigma_h}+\alpha\right)\frac{\partial \overline{t^2}}{\partial r}\right\}+2\alpha_t\left(\frac{\partial \bar{T}}{\partial r}\right)^2-2\varepsilon_t-2\alpha\left(\frac{\partial \sqrt{\overline{t^2}}}{\partial r}\right)^2 \quad (10)$$

$$\bar{u}\frac{\partial \varepsilon_t}{\partial x}+\bar{v}\frac{\partial \varepsilon_t}{\partial r}=\frac{1}{r}\frac{\partial}{\partial r}\left\{r\left(\frac{\alpha_t}{\sigma_\phi}+\alpha\right)\frac{\partial \varepsilon_t}{\partial r}\right\}+C_{P1}f_{P1}\alpha_t\frac{\varepsilon_t}{\overline{t^2}}\left(\frac{\partial \bar{T}}{\partial r}\right)^2+C_{P2}f_{P2}\nu_t\frac{\varepsilon_t}{k}\left(\frac{\partial \bar{u}}{\partial r}\right)^2$$
$$-C_{D1}f_{D1}\frac{\varepsilon_t^2}{\overline{t^2}}-C_{D2}f_{D2}\frac{\varepsilon\varepsilon_t}{k}+\alpha\alpha_t(1-f_\lambda)\left(\frac{\partial^2 \bar{T}}{\partial r\partial r}\right)^2, \quad (11)$$

respectively. The empirical constants and model functions in equations (7), (10) and (11) are summarized in Table II.

Numerical scheme

The numerical technique is based on the control volume finite-difference procedure developed by Patankar[22]. The size of non-uniform cross-stream grids

C_μ	C_1	C_2	σ_k	σ_ε	f_1	f_2	f_μ
0.09	1.45	1.9	1.0	1.3	1.0	$1\text{-}03\exp(-R_t^2)$	$\{1-\exp(\frac{R_\tau}{26.5})\}^2$

Table I. Empirical constants and model functions in the k-ε model

C_λ	C_{P1}	C_{P2}	σ_h	σ_ϕ	C_{D1}	C_{D2}	f_{P1}	f_{P2}	f_{D1}	f_{D1}	f_λ
0.11	1.80	0.72	1.0	2.20	0.80	1.0	1.0	1.0	1.0	1.0	$\{1-\exp(-\frac{\sqrt{Pr}}{30.5}\frac{2}{f}\,St\,y^+)\}$

Table II. Empirical constants and model functions in the two-equation heat transfer model

is increased with a geometric ratio from the wall towards the central region of the concentric annulus. It is used in the calculation of turbulent boundary layers to cope with large gradients near the wall surface. In order to assure the accuracy of calculated results, at least two control volumes must be located in the viscous sub-layer. Throughout numerical calculations, the number of control volumes is properly selected between 42 and 93 to obtain a grid-independent solution, resulting in no appreciable difference between the numerical results with different grid spacing. The discretized equations are solved from the inlet in the downstream direction by means of a marching procedure, since equations are parabolic. The maximum stepsize in the streamwise direction is limited to five times the minimum size in the radial direction of the control volume. At each axial location, the pressure gradient $d\bar{P}/dx$ in equation (2) is corrected at every iteration so that equation (1) is satisfied.

The hydrodynamically, fully-developed, annular flow with the inner cylinder at rest is assumed only at the starting point of the heating section. The following boundary conditions are used at the wall: at $r = R_{in}$ (inner cylinder wall): at $r = R_{in}$ (inner cylinder wall):

$$\bar{u}=U,\ k = \varepsilon = \overline{t^2} = \varepsilon_t = 0,$$
$$-\frac{\partial \bar{T}}{\partial r}=\frac{q_w}{\lambda_w}$$

at $r = R_{out}$ (outer cylinder wall):

$$\bar{u} = k = \varepsilon = \overline{t^2} = \varepsilon_t = 0,$$
$$\frac{\partial \bar{T}}{\partial r}=0 \quad \text{(insulation)}$$

Here, U denotes the velocity of the inner cylinder.

The procedure is repeated until the convergence criterion

$$\text{maximum}\left[\frac{\phi^{M}-\phi^{M-1}}{\phi^{M-1}_{max}}\right]<1X10^{-4} \tag{12}$$

is satisfied for all the variables ϕ ($\bar{u}$, $\bar{T}$, k, ε, $\overline{t^2}$ and ε_t. The superscripts M and $(M-1)$ in equation (12) indicate two successive iterations, while the subscript "max" refers to a maximum value over the entire field of iterations. The governing parameters are varied: Reynolds number Re = 10,000, 20,000, 40,000, 60,000, 80,000 and 100,000; velocity ratio N = 0, 0.5 and 1.0; and radius ratio R_{in}/R_{out} = 0.2, 0.5 and 0.8. Numerical computations were performed on a NEC personal computer (32 bit).

In order to verify the k-ε turbulence and the two-equation heat-transfer models and to determine the reliability of the computer code, numerical

predictions are compared with some existing experimental results in both the thermal and flow fields. The models are applied to a flow in an annulus (R_{in}/R_{out} = 0.56) with a stationary inner cylinder with a uniform wall heat flux. Numerical results are obtained at a location of 220 times the tube diameter downstream from the inlet where both thermally- and hydrodynamically-fully developed conditions prevail.

Figure 2 illustrates both the friction factor f and the Nusselt number Nu as a function of the Reynolds number Re. Dalle Donne and Meerwald[23] derived the correlation equations for the Nusselt number and friction factor at the inner wall of the annulus as

$$Nu = 0.020Re^{0.8}Pr^{0.4}, \quad (13)$$

$$f = 0.057Re^{-0.22} \quad (14)$$

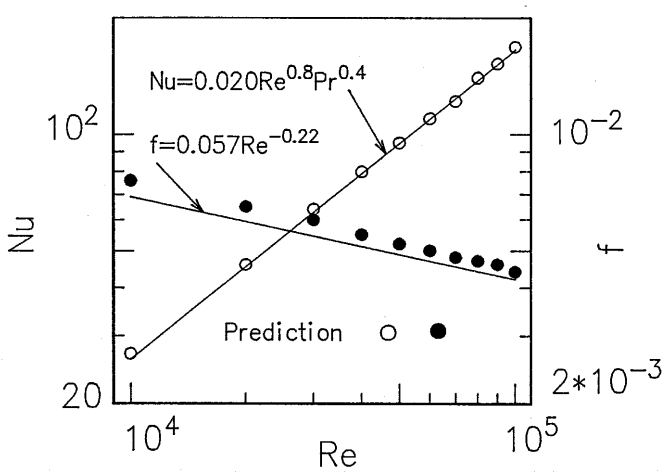

Figure 2. A comparison of predicted Nusselt number and friction factor with test results[23] for the fully-developed turbulent annular flow with a stationary inner cylinder for R_{in}/R_{out} = 0.56, x/D = 220 and Re = 46,000

The two equations are presented in Figure 2 as solid lines. Predicted values are given as hollow circles for Nu and solid circles for f. It is seen that the prediction is in good agreement with the experiments.

Figure 3 depicts the time-averaged streamwise velocity distributions obtained by means of the model together with the experimental data at Re = 46,000 obtained by Brighton and Jones[1]. Here, Figures 3(a) and (b) correspond to the distributions from the inner and outer walls to the location of the maximum streamwise velocity, respectively. The calculation result agrees with the experimental results, representing the well-known characteristics in the logarithmic region.

In Figure 4, the calculated turbulent kinetic energy is compared with the experimental data[1] at Re = 46,000. The predicted results are normalized by the square of the friction velocity on the outer wall, $(u^*_{out})^2$. The turbulence model predicts well in the outer region, but its accuracy deteriorates near the inner

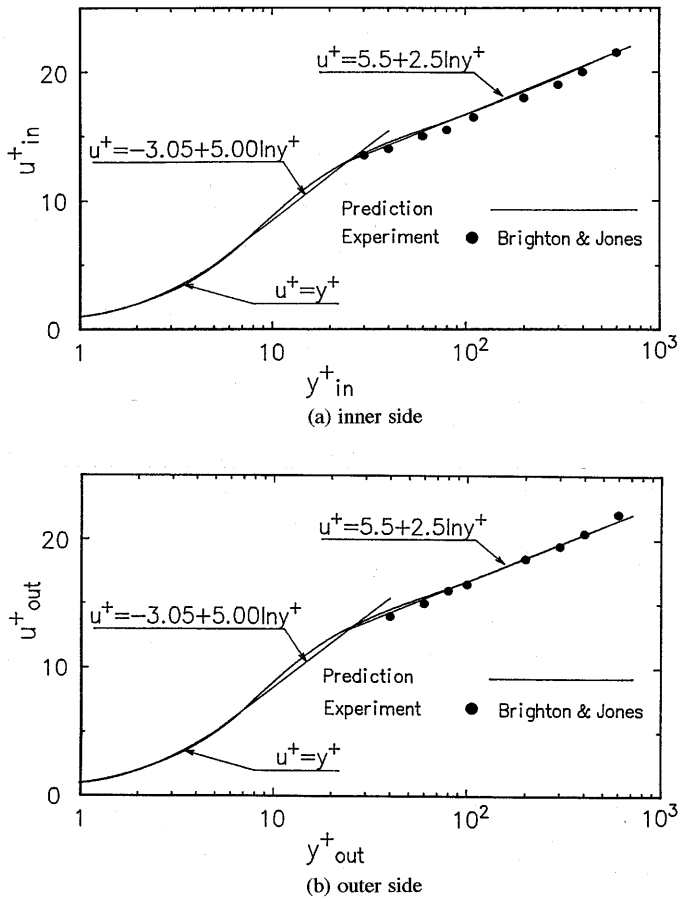

Figure 3.
A comparison of the theoretical and experimental results for radial distribution of time-averaged streamwise velocity in a stationary concentric annulus for Re = 46,000 and R_{in}/R_{out} = 0.56

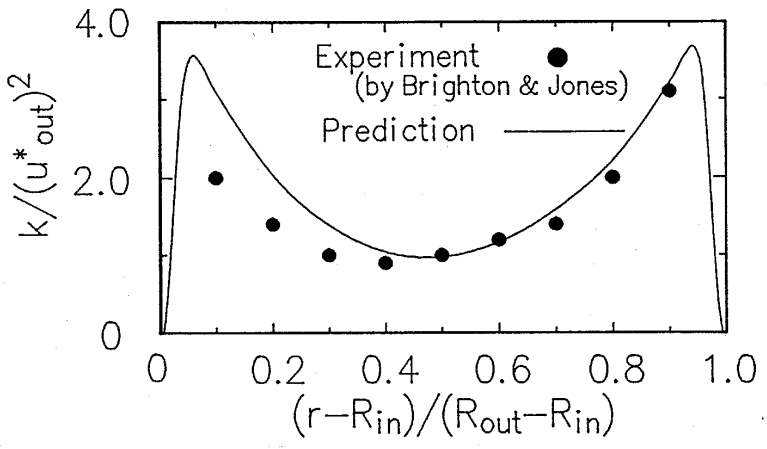

Figure 4.
A comparison of theoretical and experimental results for radial distribution of turbulent kinetic energy in a stationary concentric annulus for Re = 46,000 and R_{in}/R_{out} = 0.56

wall. That is, the turbulent kinetic energy is overestimated in the vicinity of the inner core.

The predicted radial distribution of the time-averaged temperature in the inner wall region at Re = 46,000 is illustrated in Figure 5 in the form of T^+_{in} versus Y^+_{in}. Y^+_{in} denotes the dimensionless distance measured from the heated inner wall. It is observed that the two-equation heat transfer model reproduces the law of the wall for a thermal boundary layer. The validity of the computer code and the validity of both the k-ε turbulence and two-equation heat transfer models are borne out through the above comparisons.

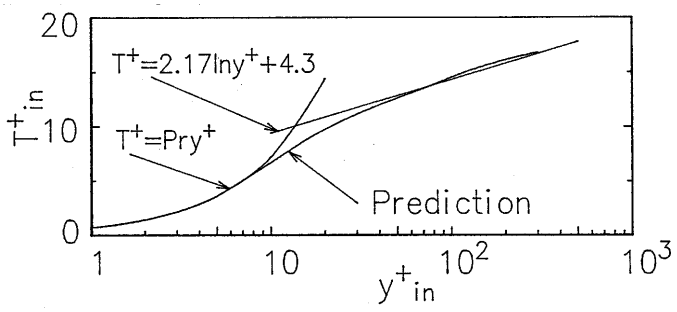

Figure 5.
Dimensionless time-averaged temperature distribution in a stationary concentric annulus for Re = 46,000 and R_{in}/R_{out} = 0.56

Results and discussion

The prediction of the Nusselt number for R_{in}/R_{out} = 0.8 is plotted against the Reynolds number in Figure 6 as a function of the velocity ratio of the moving inner cylinder to the fluid flow, N. N = 0 corresponds to the stationary ease in which heat transfer performance takes the form of

$$Nu = 0.023\, Re^{0.8} Pr^{0.4} \tag{15}$$

Likewise, heat transfer performance for a moving inner cylinder (N > 0) follows an expression similar to equation (15) as

$$Nu = C\, Re^{0.8} Pr^{0.4} \tag{16}$$

Here, C is an empirical constant which varies with the dimensionless relative velocity of the inner core N. This implies that the structure of turbulence induced by the inner core moving at certain velocity varies in a similar fashion as the Reynolds number changes. This observation is supported by Torii and Yang[13, 14], who employ the turbulent Prandtl number to determine the turbulent thermal diffusivity α_t. Figure 7 plots Nu/Nu_o against R_{in}/R_{out} at Re = 10,000. Here, Nu_o denotes the Nusselt number for a fully-developed turbulent annular flow with a stationary inner cylinder. One observes that Nu/Nu_o. decreases with an increase in the dimensionless relative velocity N and that for a given value of N, Nu/Nu_o diminishes slightly with an increase in the radius ratio R_{in}/R_{out}. It is found that a substantial reduction in the Nusselt number observed in Figure 6 is attributed to the inner core movement in the flow direction, and that this trend is induced by the dimensionless relative velocity.

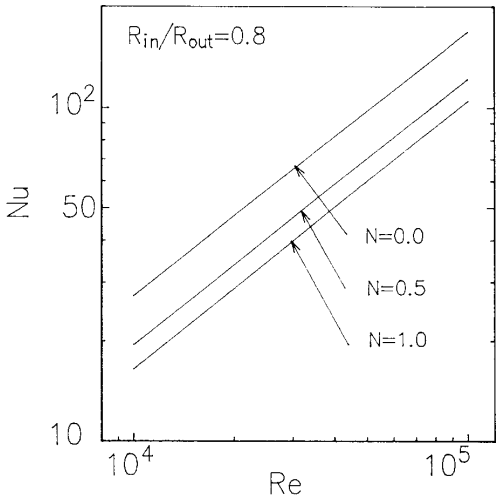

Figure 6.
Variation of predicted Nusselt number with Reynolds number as a function of dimensionless relative velocity R_{in}/R_{out} = 0.8 and x/D = 220

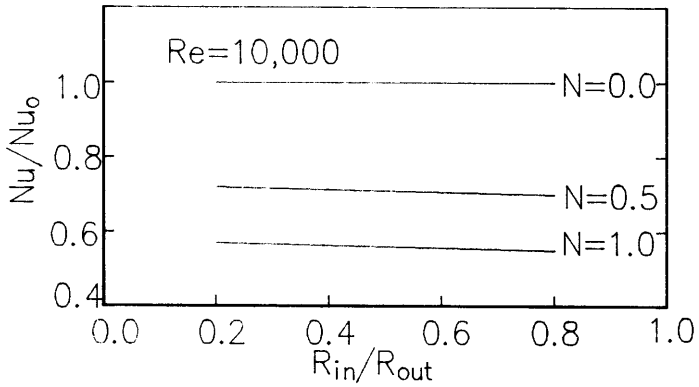

Figure 7.
Variation of predicted Nusselt numbers in a concentric annulus with three different dimensionless relative velocities for Re = 10,000 and x/D = 220

An attempt is made to explore the mechanisms of turbulent transport phenomena based on numerical results at R_{in}/R_{out} = 0.8 and Re = 10,000. Since at each value of R_{in}/R_{out}, same numerical results were obtained for different Reynolds numbers. Figure 8 illustrates the radial profile of the time-averaged streamwise velocity $\overline{u}/\overline{u}_{max}$ for three different values of the dimensionless relative velocity, N. They are normalized using the maximum value $\overline{u}_{max}$ at each respective relative velocity. It is observed that as N is increased, the peak of $\overline{u}/\overline{u}_{max}$ shifts towards the inner cylinder side, resulting in a substantial deformation of the velocity profile of the fully developed turbulent annular flow from the stationary inner cylinder case. This implies that the velocity gradient at the inner wall is significantly diminished by the streamwise movement of the inner cylinder, with only a slight change in the outer wall region.

The corresponding variation of the turbulent kinetic energy with a change in N is illustrated in Figure 9 in the same manner as Figure 4. One observes that

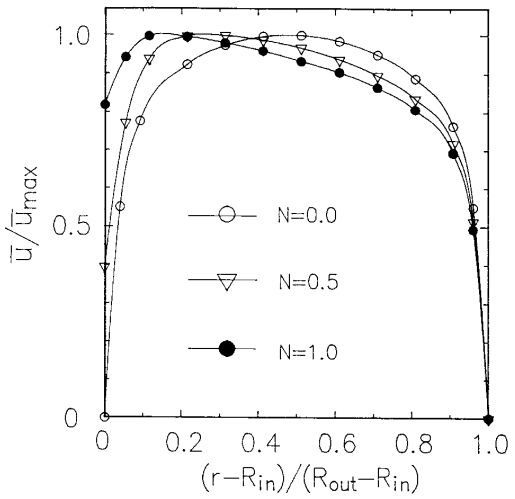

Figure 8.
Variation of time-averaged streamwise velocity profiles with three different dimensionless relative velocities for Re = 10,000 and R_{in}/R_{out} = 0.8

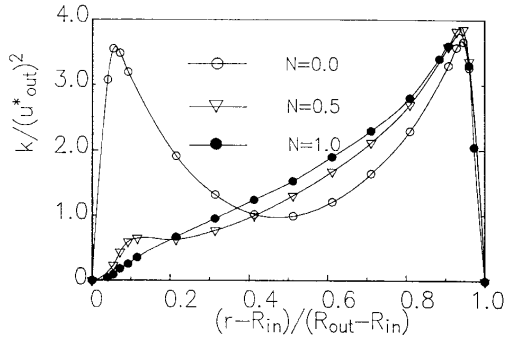

Figure 9.
Variation of turbulent kinetic energy profiles with three different dimensionless relative velocities for Re = 10,000 and R_{in}/R_{out} = 0.8

the turbulent kinetic energy level in the inner wall region is greatly reduced with an increase in N. On the contrary, the turbulent kinetic energy in the central region of the annulus increases somewhat, while no effect appears in the vicinity of the outer wall.

The radial distribution of the temperature variance, $\overline{t^2}$, in the thermal field is illustrated in Figure 10 as a function of N. Here, the temperature variance is normalized by the square of the friction temperature, t^*, for the annular flow in the absence of the inner core movement. The predicted $\overline{t^2}$ for the stationary inner core case undergoes a sharp rise in the inner wall region followed by a gradual decline towards the outer wall. As N increases, a reduction in $\overline{t^2}$ appears in the whole region of the flow cross-section and the peak is significantly diminished.

The predicted change in the turbulent heat flux profiles with the inner core movement (i.e. N) is depicted in Figure 11. The turbulent heat flux level in the vicinity of the inner wall is substantially reduced with an increase in N. The radial

distribution of the time-averaged temperature in the inner region is depicted in Figure 12 in the same manner as Figure 5 for N = 0, 0.5 and 1.0. It is observed that as the relative velocity is increased, the temperature profile deviates from the law of the wall and gradually approaches the laminar one ($T^+ = Pry^+$). This behaviour

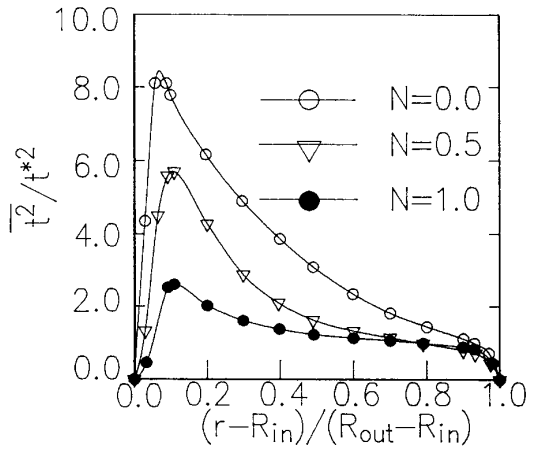

Figure 10.
Variation of temperature variance profiles with three different dimensionless relative velocities for Re = 10,000 and R_{in}/R_{out} = 0.8

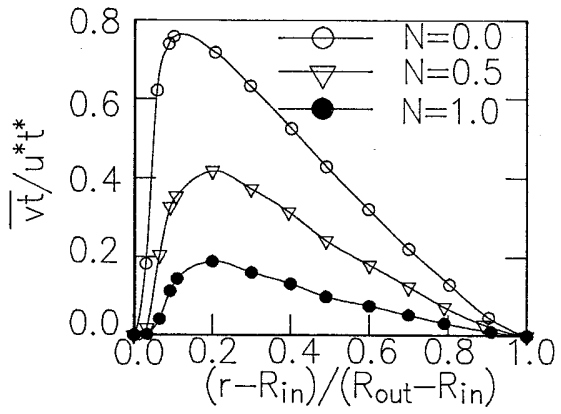

Figure 11.
Variation of turbulent heat flux profiles with three different dimensionless relative velocities for Re = 10,000 and R_{in}/R_{out} = 0.8

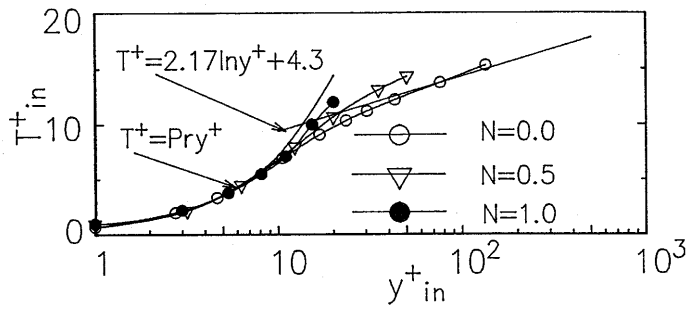

Figure 12.
Variation of time-averaged temperature profiles with three different dimensionless relative velocities for Re = 10,000 and R_{in}/R_{out} = 0.8

is in accord with the variation of the turbulent heat flux. In other words, the change in the temperature profile corresponds to the variations of the turbulent kinetic energy and the temperature variance. Since the eddy diffusivity concept (equation (5)) is employed to determine the turbulent heat flux, $-\overline{v't'}$ in equation (3), it is directly related to k, ε, $\overline{t^2}$ and ε_t in equation (7). Hence, reductions in the turbulent kinetic energy and the temperature variance cause an attenuation in the Nusselt number, as shown in Figure 6.

In summary, a decrease in the Nusselt number, as seen in Figure 6, is caused by the streamwise movement of the inner cylinder. This trend is amplified with an increase in the relative velocity. The mechanism is that

(1) in the region near the inner cylinder, a reduction in the velocity gradient induced by core movement suppresses the production of the turbulent kinetic energy and the temperature variance; and

(2) it induces an attenuation in the turbulent thermal diffusivity, i.e. a decrease in the turbulent heat flux, resulting in the deterioration of heat transfer performance.

Conclusions

The two-equation model for heat transfer and the turbulence model have been employed to numerically investigate the fluid flow and heat transfer phenomena in a concentric annulus with a slightly heated inner core moving in the flow direction. Consideration is given to the influence of the relative velocity on the flow and thermal fields. The following conclusions are derived from the present study:

The present heat transfer model predicts a reduction in the Nusselt number with an increase in the velocity ratio of the moving inner cylinder and the fluid flow. It is disclosed that:

(1) the velocity gradient in the vicinity of the inner core wall is decreased due to its streamwise movement;

(2) the turbulent kinetic energy and the temperature variance are substantially reduced in the inner region, resulting in an attenuation in the turbulent heat flux; and

(3) the radial profile of the time-averaged temperature gradually approaches the laminar one. Consequently, the turbulent kinetic energy and the temperature variance in the region near the inner wall are substantially suppressed due to the streamwise movement of the inner cylinder, resulting in the deterioration of heat transfer performance.

References

1. Brighton, J.A. and Jones, J.B., "Fully developed turbulent flow in annuli", *Transactions of ASME,* D, 1964, pp. 835-44.
2. Kays, W.M. and Leung, E.Y., "Heat transfer in annular passages (hydrodynamically developed turbulent flow with arbitrarily prescribed heat flux", *International Journal of Heat Mass Transfer,* Vol. 6, 1963, pp. 537-57.

3. Heikal, M.R.F., Walkalate, P.J. and Hatton, A.P., "The effect of free stream turbulence level on the flow and heat transfer in the entrance region of an annulus", *International Journal of Heat Mass Transfer*, Vol. 20, 1977, pp. 763-71.
4. Fujii, S., Akino, N., Hishida, M., Kawamura, H. and Sanokawa, K., "Experimental and theoretical investigations on heat transfer of strongly heated turbulent gas flow in an annular duct", *JSME International Journal, Series II*, Vol. 34 No. 3, 1991, pp. 348-54.
5. Torii, S, Shimizu, A., Hasegawa, S. and Higasa, M., "Laminarization of strongly heated annular gas flows", *JSME International Journal, Series. II*, Vol. 34 No. 2, 1991, pp. 157-68.
6. Kuzay, T.M. and Scott, C.J., "Turbulent heat transfer studies in annulus with inner cylinder rotation", ASME Paper No. 75WA/HT-55, 1975.
7. Kuzay, T.M. and Scott, C.J., "Turbulent Prandtl numbers for fully developed rotating annular axial flow of air", ASME Paper No. 76-HT-36, 1976.
8. Hirai, S., Takagi, T., Tanaka, K. and Kida, K., "Effect of swift on the turbulent transport of momentum in a concentric annulus with a rotating inner cylinder", *Transactions of JSME*, Vol. 53 No. 486, 1987, pp. 432-7.
9. Torii, S. and Yang, W.-J., "A numerical study on turbulent flow and heat transfer in circular Couette flows", *Numerical Heat Transfer*, Part A, Vol. 26, 1994, pp. 231-336.
10. Barrow, H. and Pope, C.W., "A simple analysis of flow and heat transfer in railway tunnels", *Heat and Fluid Flow*, Vol. 8, 1987, pp. 119-23.
11. Lee, Y. and Kim, K.H., "Inverted annular film boiling", *International Journal of Multiphase Flow*, Vol. 13, 1987, pp. 345-55.
12. Shigechi, T., Kawae, N. and Lee, Y., "Turbulent fluid flow and heat transfer in concentric annuli with moving cores", *International Journal of Heat Mass Transfer*, Vol. 33 No. 9, 1990, pp. 2029-37.
13. Torii, S. and Yang, W.-J., "A numerical study turbulent Couette flow and heat transfer in concentric annuli", *International Journal of Numerical Methods for Heat & Fluid Flow*, Vol. 4, 1994, pp. 367-77.
14. Torii, S. and Yang, W.-J., "A numerical study on turbulent Couette flow and heat transfer in concentric annuli by means of a Reynolds stress turbulence mode", *International Journal of Rotating Machinery,* 1994.
15. Launder, B.E. and Shima, N., "Second-moment closure for the near-wall sub-layer: development and application", *AIAA, Journal,* Vol. 27 No. 10, 1989, pp. 1,319-25.
16. Hishida, M., Nagano, Y. and Tagawa, M., *Heat Transfer*, Vol. 3, Hemisphere, Washington, DC, 1986, pp. 925-34.
17. Kasagi, N., Tomita, Y. and Kuroda, A., "Direct numerical simulation of passive scalar field in a turbulent channel flow", *Journal of Heat Transfer*, Vol. 114, 1992, pp. 598-606.
18. Sinh, T.H. and Lumly, J.L., "Influence of time scale ratio on scalar flux relaxation: modelling Sirivat & Warhaft's homogeneous passive scalar fluctuations", *Journal of Fluids Mechanics,* Vol. 162, 1986, pp. 211-22.
19. Nagano, Y. and Kim. C., "A two-equation model for heat transport in wall turbulent shear flows", *Journal of Heat Transfer*, Vol. 110, 1988, pp. 583-9.
20. Rodi, W., "Examples of turbulence models for incompressible flows", *AIAA, Journal*, Vol. 20, 1982, pp. 872-9.
21. Nagano, Y. and Hishida, M., "Improved form of the model for wall turbulent shear flows", *Transactions of ASME, Service D*, Vol. 109, 1987, pp. 156-60.
22. Patankar, S.V., *Numerical Heat Transfer and Fluid Flow*, Hemisphere, Washington, DC, 1980.
23. Dalle Donne, M. and Meerwald, E., "Experimental local heat transfer and average friction coefficients for subsonic turbulent flow of air in an annulus at high temperatures", *International Journal Heat Mass Transfer*, Vol. 9, 1966, pp. 1361-76.